A&A 574, A80 (2015)
DOI: 10.1051/0004-6361/201424888

Astronomy & Astrophysics

High-resolution CRIRES spectra of Terzan 1: a metal-poor globular cluster toward the inner bulge⋆

E. Valenti[1], L. Origlia[2], A. Mucciarelli[3], and R. M. Rich[4]

[1] European Southern Observatory, Karl-Schwarzschild-Str. 2, 85748 Garching bei Muenchen, Germany
e-mail: evalenti@eso.org
[2] INAF – Osservatorio Astronomico di Bologna, via Ranzani 1, 40127 Bologna, Italy
e-mail: livia.origlia@oabo.inaf.it
[3] University of Bologna, Physics & Astronomy Dept., viale Berti Pichat 6-2, 40127 Bologna, Italy
[4] Physics and Astronomy Bldg, 430 Portola Plaza Box 951547 Department of Physics and Astronomy, University of California at Los Angeles, Los Angeles, CA 90095-1547, USA

Received 31 August 2014 / Accepted 20 November 2014

ABSTRACT

Aims. Containing the oldest stars in the Galaxy, globular clusters toward the bulge can be used to trace its dynamical and chemical evolution. In the bulge direction, there are ∼50 clusters, but only about 20% have been subject of high-resolution spectroscopic investigations. So far, the sample observed at high resolution spans a moderate-to-high metallicity regime. In this sample, however, very few are located in the innermost region ($R_{GC} \leq 1.5$ Kpc and $|l, b| \leq 5°$). To constrain the chemical evolution enrichment of the innermost region of Galaxy, accurate abundances and abundance patterns of key elements based on high-resolution spectroscopy are necessary. Here we present the results we obtained for Terzan 1, a metal-poor cluster located in the innermost bulge region.
Methods. Using the near-infrared spectrograph CRIRES at ESO/VLT, we obtained high-resolution ($R \approx 50\,000$) H-band spectra of 16 bright giant stars in the innermost region ($r \leq 60''$) of Terzan 1. Full spectral synthesis techniques and equivalent width measurements of selected lines, isolated and free of significant blending and/or contamination by telluric lines, allowed accurate chemical abundances and radial velocities to be derived.
Results. Fifteen out of 16 observed stars are likely cluster members, with an average heliocentric radial velocity of $+57 \pm 1.8$ km s^{-1} and mean iron abundance of [Fe/H] = -1.26 ± 0.03 dex. For these stars we measured some [α/Fe] abundance ratios, finding average values of [O/Fe] = $+0.39 \pm 0.02$ dex, [Mg/Fe] = $+0.42 \pm 0.02$ dex, [Si/Fe] = $+0.31 \pm 0.04$ dex, and [Ti/Fe] = $+0.15 \pm 0.04$ dex
Conclusions. The α enhancement (≈+ 0.4 dex) found in the observed giant stars of Terzan 1 is consistent with previous measurements on other, more metal-rich bulge clusters, which suggests a rapid chemical enrichment.

Key words. techniques: spectroscopic – stars: abundances – stars: Population II – globular clusters: individual: Terzan 1 – infrared: stars

1. Introduction

Observational and theoretical studies have long shown that Galactic globular clusters (GCs) contain the oldest stars in the Galaxy. They represent an important tracer of the underlying population, therefore deriving accurate abundances and abundance patterns in GCs represents a crucial test for tracing the early dynamical and chemical evolution of the Galaxy. The elemental abundance distributions and the abundance ratio of certain critical elements, such as Fe-peak, CNO, and α-elements (i.e., those synthesized from α particles, such as O, Ne, Mg, Si, Ti, Ca and S) are particularly suitable for this purpose. Indeed, these elements are synthesized in stars of different masses, hence released into the interstellar medium on different timescales. A particularly useful abundance ratio is [α/Fe]. Thanks to the time delay in the bulk of Fe production relative to α-elements, the [α/Fe] abundance ratio can be efficiently used as a cosmic clock (see, e.g., McWilliam 1997).

An overall [α/Fe] enhancement with respect to the solar value has been well established in the Galactic halo GCs population for several years (see Gratton et al. 2004, for a general review), indicating a major enrichment by type II SNe on a short timescale. On the other hand, accurate abundance patterns are only available for some GCs in the bulge direction. Within a total population of about 50 GCs located in the bulge (Harris 1996, 2010 compilation), only about 20% have been subject to spectroscopic investigation at moderately high spectral resolution ($R \geq 20\,000$) for detailed chemical abundance analysis. Our team has contributed significantly to this subject by measuring chemical abundances in cool giants that are members of 12 bulge GCs (Origlia et al. 2002, 2005a,b, 2008; Origlia & Rich 2004; Valenti et al. 2011) by using H-band high-resolution spectra obtained at KeckII with NIRSPEC (McLean 1998). Chemical abundances from high-resolution optical spectroscopy in seven other bulge GCs have been obtained by Barbuy et al. (1999, 2006, 2007, 2014); Cohen et al. (1999); Carretta et al. (2001, 2007); Zoccali et al. (2004); Alves-Brito et al. (2006); Gratton et al. (2006).

From the measured Fe, O, Ti, Si, Mg, and Ca abundances, we found that the [α/Fe] ratios are enhanced by a factor between 2 and 3 over the whole range of metallicity spanned by the observed clusters. All these measurements indicate that the bulk of the bulge GC population probably formed from a gas that is mainly enriched by type II SNe and on a short timescale, before substantial contribution of type Ia SNe took place.

⋆ Based on data taken at the ESO/VLT Telescope, within the observing program 093.D-0179(A).

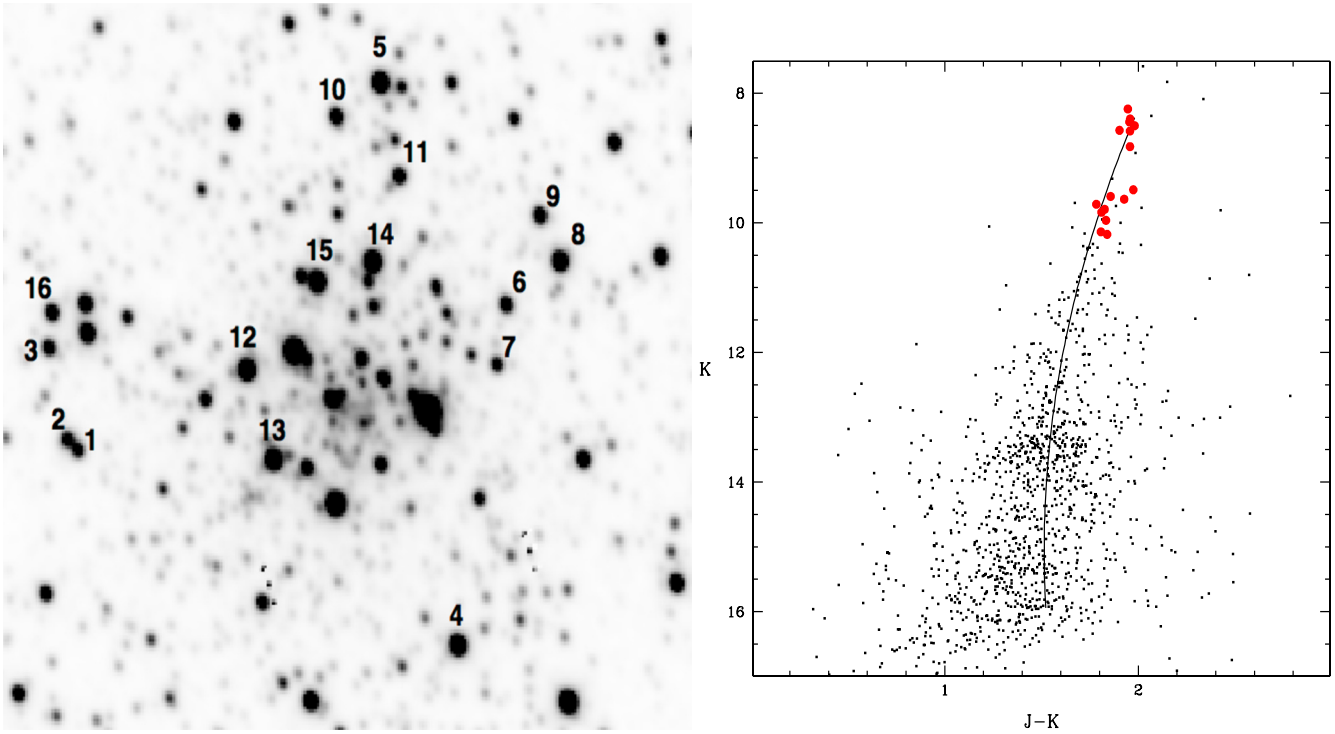

Fig. 1. *Left panel*: sofI K-band image of the core region of Ter 1. The field of view shown in the map is $\sim 1' \times 1'$, north is up and east on the left. The observed stars are numbered (cf. Table 1). *Right panel*: observed K, $(J-K)$ CMD, and mean RGB ridgeline of Ter 1 in the central $\sim$1 arcmin in radius from Valenti et al. (2010). Large red filled points denote the stars observed spectroscopically.

With the only exception of Terzan 4 (Origlia & Rich 2004), which has a metallicity [Fe/H] $= -1.6$ dex, all the bulge GCs observed so far at high spectral resolution have metallicity [Fe/H] ≥ -1.0 dex. In this sample observed at high-resolution, there are very few clusters located in the very innermost bulge region (i.e., $R_{\rm GC} \leq 1.5$ Kpc and $|l, b| \leq 5°$).

With the aim of understanding the chemical composition of the innermost stellar populations in the Galactic bulge, we used CRIRES at the VLT (Käufl et al. 2004) to measure the chemical composition of a few GCs located toward the center of the bulge. Here we present the results for Terzan 1.

Terzan 1 is a GC located close to the plane, with somewhat controversial reddening and distance estimates. An optical photometric study with HST-WFPC2 by Ortolani et al. (1999) suggested $E(B-V) = 2.48$ and $(m-M)_0 = 13.58$. A near-IR study by Valenti et al. (2010) suggested a lower reddening $E(B-V) = 1.99$ and a larger distance modulus $(m-M)_0 = 14.13$. However, when taking the different $\Delta E(B-V) = 0.5$ into account, the two distance estimates agree within the errors ($\sim$0.2 mag). From the morphology (i.e., color, magnitude, and slope) of the cluster's red giant branch (RGB) in the $(K, J-K)$ color–magnitude diagram (CMD), we derived a photometric metallicity [Fe/H] $= -1.1$ dex (Valenti et al. 2010). Low-resolution optical spectroscopy of 11 giants that are likely members of Terzan 1 which was obtained by Idiart et al. (2002, hereafter I02), suggests a [Fe/H] ≈ -1.3 and some [Mg/Fe] enhancement with respect to the solar ratio.

2. Observations and data reduction

To minimize the risk of contamination from bulge field stars, we selected 16 bright giants ($8 \leq K \leq 10.5$) using the near-IR CMD by Valenti et al. (2010) in the innermost region (at $r \leq 60''$) and along the mean RGB ridgeline (see Fig. 1). Table 1 lists the near-IR magnitude and coordinates of the selected stars, whereas Fig. 1 shows their spatial distribution within the cluster.

Observations were executed in service mode, during several nights in April and June 2014 and under an average seeing of $\approx 1''$. We used CRIRES in non-AO mode and selected a slit width of $0.4''$ providing a spectral resolution $R \approx 50\,000$ and two different gratings in the H band, namely 1550.8 nm/order#36 and 1598.0 nm/order#36. However, because of the known vignetting and noise problems affecting the four detectors, only portions of the spectra in the ranges: 1.547−1.553 μm, 1.557−1.635 μm, 1.575−1.581 μm, 1.585−1.590 μm, and 1.595−1.601 μm were actually usable.

The integration time, on source and per setting, was 20 min. The data was reduced by using the CRIRES pipeline[1], which performs sky subtraction using the pair of spectra obtained when the object is nodded along the slit and flat-fielding correction. Wavelength calibration was performed using a ThAr lamp and a second-order polynomial solution. Because of the gaps within the four CRIRES detectors and the relatively narrow wavelength range covered by each setting, the derived wavelength solution using the ThAr lamp strongly depends upon the number and distribution of available lines within a given detector. Therefore, to check and refine the pipeline wavelength solutions, we cross-correlated (using the IRAF task *fxcor*) the spectra of an O star observed for telluric correction before or after the targets, with a high-esolution spectrum of the Earth's telluric features retrieved from the ESO web page[2]. The cross-correlation between the template and the O-type star spectra was performed over a region around 1.577 μm where several telluric features are present.

[1] http://www.eso.org/sci/software/pipelines
[2] http://www.eso.org/sci/facilities/paranal/decommissioned/isaac/tools/spectroscopic_standards.html

Table 1. Stars toward Terzan 1 observed with CRIRES and selected from Valenti et al. (2010) catalog.

ID	J	H	K	RA (J2000)	Dec (J2000)
1	11.947	10.564	10.140	263.9564516	−30.4829633
2	11.796	10.392	9.963	263.9568131	−30.4826890
3	11.648	10.250	9.838	263.9574730	−30.4803350
4	10.542	9.088	8.585	263.9430320	−30.4880850
5	10.478	–	8.575	263.9457667	−30.4733797
6	11.618	10.237	9.792	263.9413450	−30.4792040
7	12.018	10.618	10.179	263.9416433	−30.4807381
8	10.783	9.294	8.826	263.9394140	−30.4780540
9	11.565	10.113	9.638	263.9401400	−30.4768680
10	11.450	10.028	9.593	263.9473110	−30.4742850
11	11.498	10.123	9.715	263.9451520	−30.4758380
12	10.398	8.960	8.444	263.9504970	−30.4808830
13	10.485	9.020	8.504	263.9495090	−30.4832320
14	10.356	8.913	8.398	263.9460670	−30.4781060
15	10.191	8.688	8.245	263.9480840	−30.4785630
16	11.466	10.045	9.492	263.9573380	−30.4793950

3. Chemical abundance analysis

To measure the chemical abundances of the RGB stars in Terzan 1 from the CRIRES spectra, we performed the same analysis as in our previous works on bulge GC and field giants (see Valenti et al. 2011; Rich et al. 2012, and references therein).

We made use of full spectral synthesis techniques and the equivalent width measurements of selected lines, which were sufficiently isolated, free of significant blending and/or contamination by telluric absorption. Telluric absorptions were carefully checked on an almost featureless O-star spectrum.

To compute suitable synthetic spectra and model the observed giant stars, we used an updated version (Origlia et al. 2002) of the code first described in Origlia et al. (1993). The code uses the LTE approximation, which is based on the molecular blanketed model atmospheres of Johnson et al. (1980) at temperatures ≤4000 K and the ATLAS9 models for temperatures above 4000 K. It includes thousands of near IR atomic transitions from the Kurucz database[3], from Biemont & Grevesse (1973), and from Melendez & Barbuy (1999). Molecular data are from our compilations (Origlia et al. 1993, and subsequent updates) and from B. Plez (priv. comm.). The reference Solar abundances are from Grevesse & Sauval (1998).

An initial guess of the temperature and gravity of the observed stars has been derived from their near-IR photometry, while for the microturbulence velocity we adopted an average value of 2.0 km s^{-1} (see also Origlia et al. 1997). These photometric estimates of the stellar parameters were used as input to produce a grid of model spectra that span a wide range in terms of abundances and abundance patterns, while keeping the stellar parameters (temparature and gravity) around the photometric values. The model that reproduces the overall observed spectrum and the equivalent widths of selected lines better was chosen as the best fit model. Equivalent widths were computed by Gaussian fitting the line profiles, with an overall uncertainty ≤10%.

We have been able to reliably measure a handful of Fe and OH lines, and (depending on the signal-to-noise of the spectra) one or two Ti, Si, and Mg lines. Equivalent width measurements of these lines were used to get abundances of Fe, O, and other three (Mg, Si, and Ti) alpha-elements. Carbon abundances are mostly determined from the 3−0 ^{12}CO bandhead by means of full spectral synthesis. A few, quite faint CN lines are also present in the spectra of the observed stars but the signal-to-noise is not adequate to get reliable nitrogen abundances.

For each observed star, Table 2 lists the final adopted photospheric parameters, the measured radial velocity, and chemical abundances. In particular, the tabulated star temperature and gravity values are photometric, but spectroscopically fine-tuned to get simultaneous spectral fitting of the CO bandhead, the OH molecular lines, and the atomic lines observed in the CRIRES spectra. The impact of using slightly different assumptions for the stellar parameters on the derived abundances is discussed in Sect. 3.1. However, it is worth mentioning that since the CO and OH molecular line profiles are very sensitive to effective temperature, gravity, and microturbulence variations, they reliably constrain the values of the photospheric parameters, therefore significantly reducing their initial range of variation and ensuring a good self-consistency of the overall spectral synthesis procedure (Origlia et al. 2002; Origlia & Rich 2004). As a clear example, Fig. 2 shows the CRIRES spectra centered on some lines of interest of two giant stars (#11 and #12) with very similar abundances but very different temperatures. The coolest giant (#12 at $T_{\rm eff}$ = 3600 K) has much deeper molecular OH and CO lines than the warmest one (#11 at $T_{\rm eff}$ = 4250 K).

3.1. Error budget

We can quantify random and systematic errors in the measurement of the equivalent widths and in the derived chemical abundances as follows. The typical random error of the measured line equivalent widths is 10%, arising mostly from a ±2% uncertainty in the placement of the pseudo-continuum, as estimated by overlapping the synthetic and the observed spectra. Such random uncertainties in the line equivalent width measurements correspond to abundance variations ranging from a few hundredths to 1 tenth of a dex. This ≤0.1 dex error is somewhat lower than the typical 1σ scatter in the derived abundances from different lines, which normally ranges between 0.1 and 0.2 dex. The errors quoted in Table 2 for the final abundances are obtained by dividing these 1σ errors by the squared root of the number of used lines. When only one line is available, a 0.1 dex value has been adopted.

Most of the systematics arise from varying the adopted stellar parameters. In order to properly quantify them, we generated a grid of test models with varying the stellar parameters within ±200 K in temperature ($T_{\rm eff}$), ±0.5 dex in log-gravity (log g) and ±0.5 km s^{-1} in microturbulence velocity (ξ), and the abundances by ± − 0.1−0.2 dex accordingly, to reproduce the line depths. As a figure of merit of the statistical test we adopt the difference between the model and the observed spectrum. To quantify systematic discrepancies, this parameter is more powerful than the classical χ^2 test, which is instead equally sensitive to random and systematic scatters (see Origlia & Rich 2004, for more discussion and references therein).

All these alternative solutions turn out to be somewhat less statistically significant (typically at $1 \leq \sigma \leq 3$ level only) than our best-fit solution ($P > 90\%$). Moreover, since the stellar features under consideration show a similar trend with variation in the stellar parameters, although with different sensitivity, *relative* abundances are less dependent on stellar parameter assumptions, reducing the systematic uncertainty to <0.15 dex.

[3] http://www.cfa.harvard.edu/amp/ampdata/kurucz23/sekur.html

Table 2. Chemical abundances of the stars toward Terzan 1 observed with CRIRES.

ID	$T_{\rm eff}$	lg g	V_r	[Fe/H]	[C/Fe]	[O/Fe]	[Mg/Fe]	[Si/Fe]	[Ti/Fe]	ID-I02[a]
1	4000	1.0	+60	−1.45 ± 0.08	−0.15 ± 0.13	+0.36 ± 0.11	+0.44 ± 0.10	–	+0.03 ± 0.13	13
2	4000	1.0	+61	−1.45 ± 0.09	−0.15 ± 0.13	+0.38 ± 0.15	+0.39 ± 0.13	–	+0.05 ± 0.13	–
3	4250	1.5	+51	−1.07 ± 0.09	−0.33 ± 0.13	+0.28 ± 0.15	+0.39 ± 0.12	–	+0.14 ± 0.13	12
4	3800	1.0	+67	−1.30 ± 0.07	−0.10 ± 0.12	+0.49 ± 0.09	+0.32 ± 0.12	+0.04 ± 0.12	+0.21 ± 0.12	5
5	3800	1.0	+53	−1.34 ± 0.06	−0.06 ± 0.12	+0.48 ± 0.09	+0.41 ± 0.12	+0.23 ± 0.12	+0.03 ± 0.12	9
6	3800	1.0	+65	−1.26 ± 0.14	−0.14 ± 0.17	+0.26 ± 0.15	+0.54 ± 0.17	+0.56 ± 0.17	+0.03 ± 0.17	–
7	4000	1.0	+56	−1.25 ± 0.08	−0.15 ± 0.13	+0.56 ± 0.08	+0.54 ± 0.13	–	+0.24 ± 0.13	6
8	3800	1.0	+73	−1.25 ± 0.11	−0.25 ± 0.15	+0.41 ± 0.12	+0.45 ± 0.16	+0.45 ± 0.15	+0.40 ± 0.15	–
9	3600	1.0	−47	−1.00 ± 0.08	−0.20 ± 0.13	+0.39 ± 0.09	+0.31 ± 0.18	+0.05 ± 0.13	–	–
10	4000	1.0	+61	−1.29 ± 0.10	−0.11 ± 0.14	+0.46 ± 0.11	+0.55 ± 0.14	+0.37 ± 0.14	+0.27 ± 0.14	–
11	4250	1.5	+50	−1.24 ± 0.04	−0.16 ± 0.11	+0.46 ± 0.07	+0.49 ± 0.11	+0.36 ± 0.11	+0.19 ± 0.11	–
12	3600	0.5	+53	−1.26 ± 0.10	−0.14 ± 0.14	+0.41 ± 0.11	+0.33 ± 0.15	+0.23 ± 0.14	+0.02 ± 0.14	4
13	3600	0.5	+50	−1.21 ± 0.06	−0.19 ± 0.12	+0.26 ± 0.10	+0.25 ± 0.12	–	–	–
14	3600	0.5	+47	−1.18 ± 0.11	−0.32 ± 0.15	+0.33 ± 0.13	+0.39 ± 0.15	+0.20 ± 0.15	–	7
15	3600	0.5	+58	−1.22 ± 0.04	−0.18 ± 0.11	+0.38 ± 0.05	+0.46 ± 0.11	+0.33 ± 0.11	+0.03 ± 0.11	–
16	4000	1.0	+54	−1.20 ± 0.12	−0.20 ± 0.16	+0.37 ± 0.14	+0.41 ± 0.18	+0.36 ± 0.16	+0.32 ± 0.16	11

Notes. [(a)] Stars in common with I02 sample. The star reference identification is taken from their Table 3.

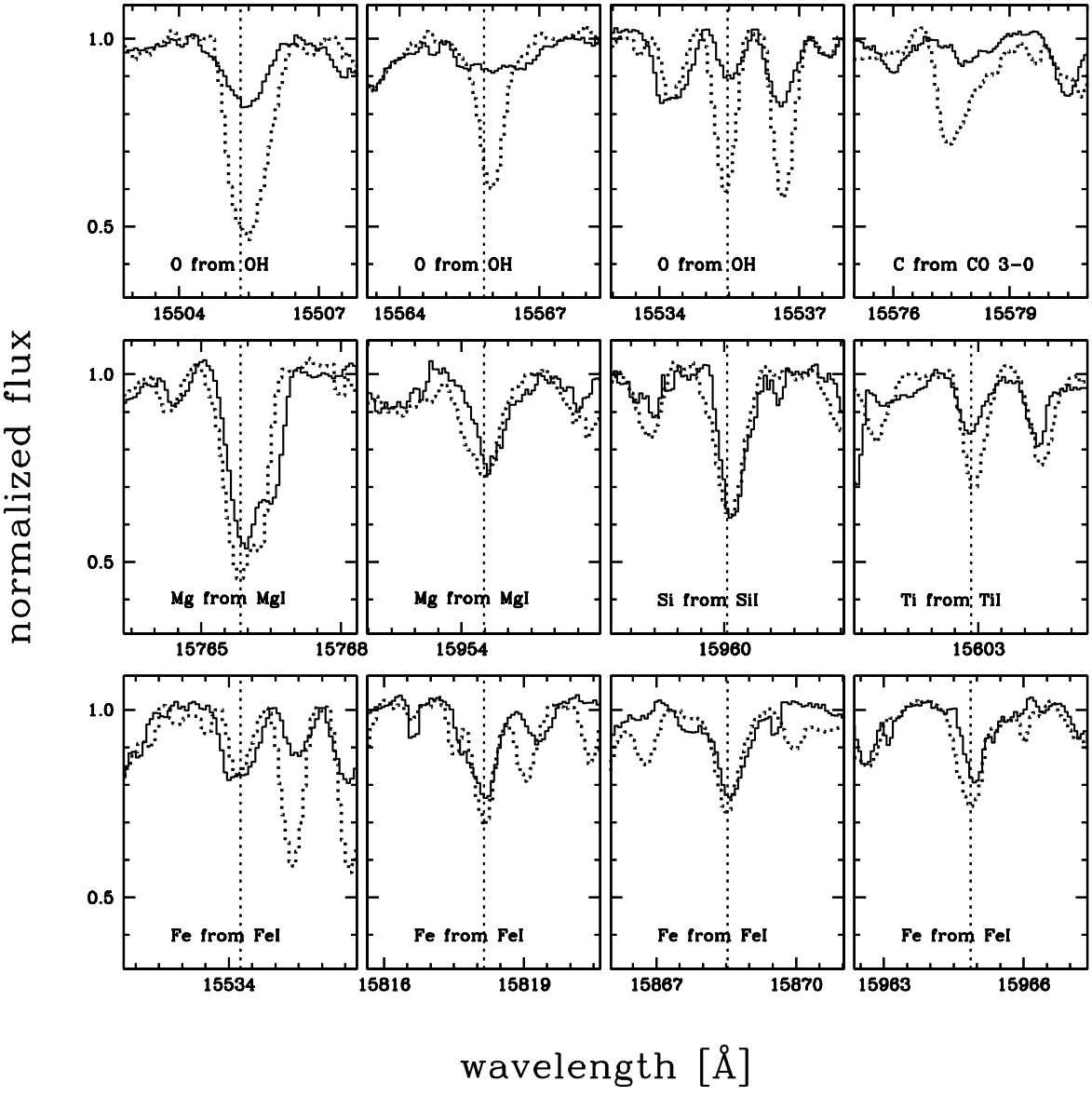

Fig. 2. CRIRES spectra centered on some lines of interest of two giant stars (#11, continous line and #12, dotted line) with very similar abundances but very different temepratures. The coolest giant (#12 at $T_{\rm eff}$ = 3600 K) has much deeper molecular OH and CO lines than the warmest one (#11 at $T_{\rm eff}$ = 4250 K).

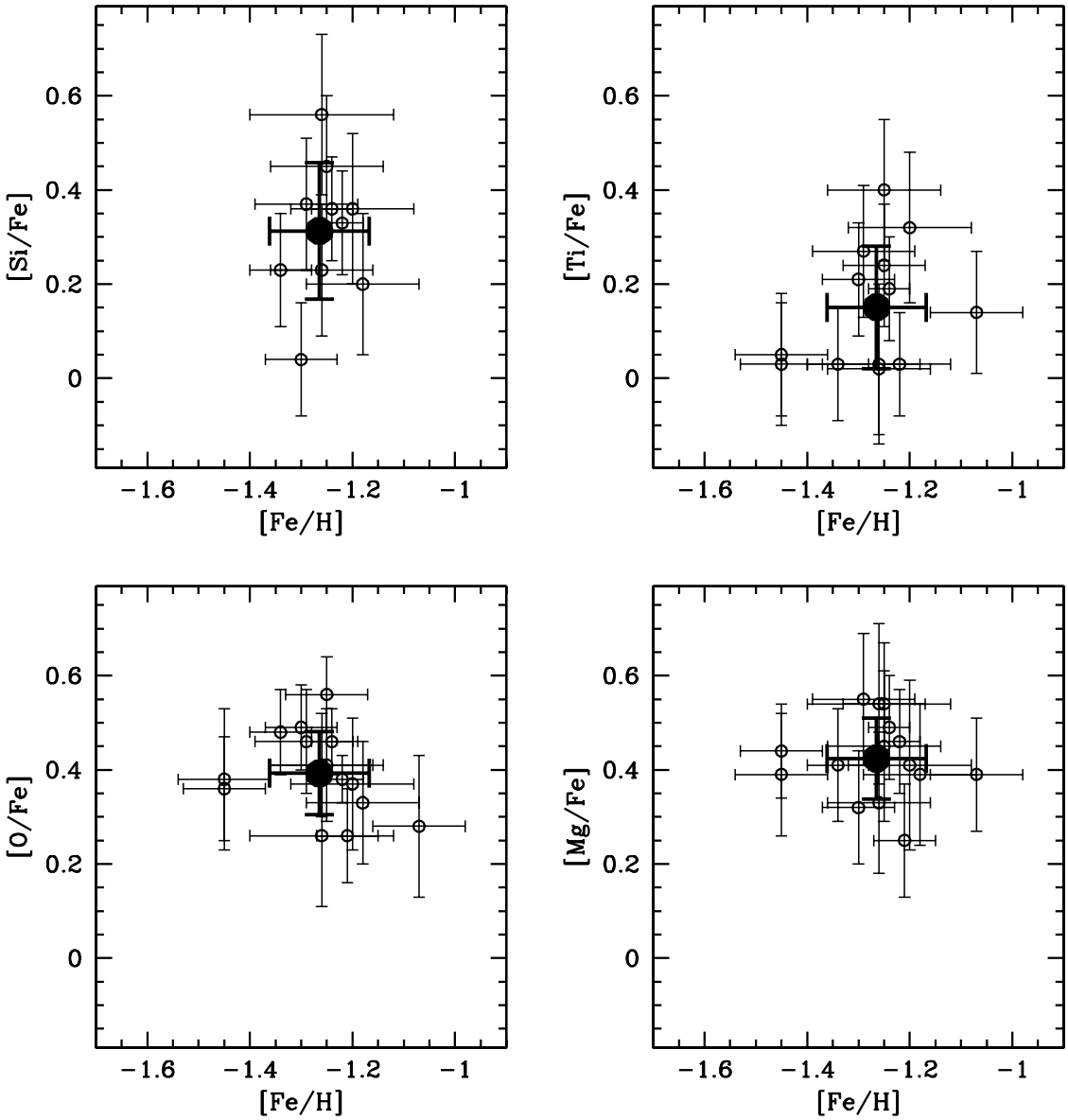

Fig. 3. [α/Fe] abundance ratios as a function of [Fe/H] for the 15 stars likely cluster members. The big dots indicate the average values and 1σ dispersions.

4. Results and discussion

For all of the 16 stars observed with CRIRES, Table 2 lists the measurement of the radial velocities and abundances. The typical random error in the radial velocity estimate is ≈1 km s^{-1}. Fifteen out of the 16 stars show heliocentric radial velocities consistent with being clustered around an average value of +57 km s^{-1} with 1σ dispersion of 7 km s^{-1}. The 15 stars with similar radial velocities also show very similar iron abundances, with an average [Fe/H] = −1.26 ± 0.03 dex and 1σ dispersion of 0.10 ± 0.02 dex. For the same stars we also measured some [α/Fe] abundance ratios, finding average values of [O/Fe] = +0.39 ± 0.02 dex (σ = 0.09 ± 0.02 dex), [Mg/Fe] = +0.42 ± 0.02 dex (σ = 0.09 ± 0.02 dex), [Si/Fe] = +0.31 ± 0.05 dex (σ = 0.15 ± 0.03 dex), and [Ti/Fe] = +0.15 ± 0.04 dex (σ = 0.13 ± 0.03 dex). Figure 3 shows the measured [α/Fe] abundance ratios as a function of [Fe/H]. These values of [α/Fe] are fully consistent with those normally observed in the bulge stars: an enhancement of a factor of ∼2−3 with respect to the solar value up to about solar metallicity. We also measured carbon abundances, finding an average [C/Fe] = −0.18 ± 0.02 dex and 1σ disperison of 0.08 ± 0.02 dex. Some depletion of the [C/Fe] abundance ratio with respect to the solar value is normally observed in low-mass giant stars that are brighter than the RGB bump.

As shown in Fig. 4, there is no evidence for any specific trend between the measured radial velocity and metallicity or distance from the cluster center, making all the 15 stars reasonable cluster member candidates. Only one star (#9) in our sample shows a radial velocity significantly different (by −104 km s^{-1}) from the average value of +57 km s^{-1} shown by the 15 other stars, thus making it a candidate field star. Moreover, this star also has a metal content that is higher by about a factor of 3.

Eight stars in our sample (see Table 2) have previously been observed by I02 at low resolution ($R \leq 2000$) in the optical range (λ4800−6600 Å and λ3980−7848 Å). It is worth mentioning, however, that because the coordinates of such stars were not published by I02, the cross-identification is based on visual inspection of their Fig. 1, showing the position of the observed

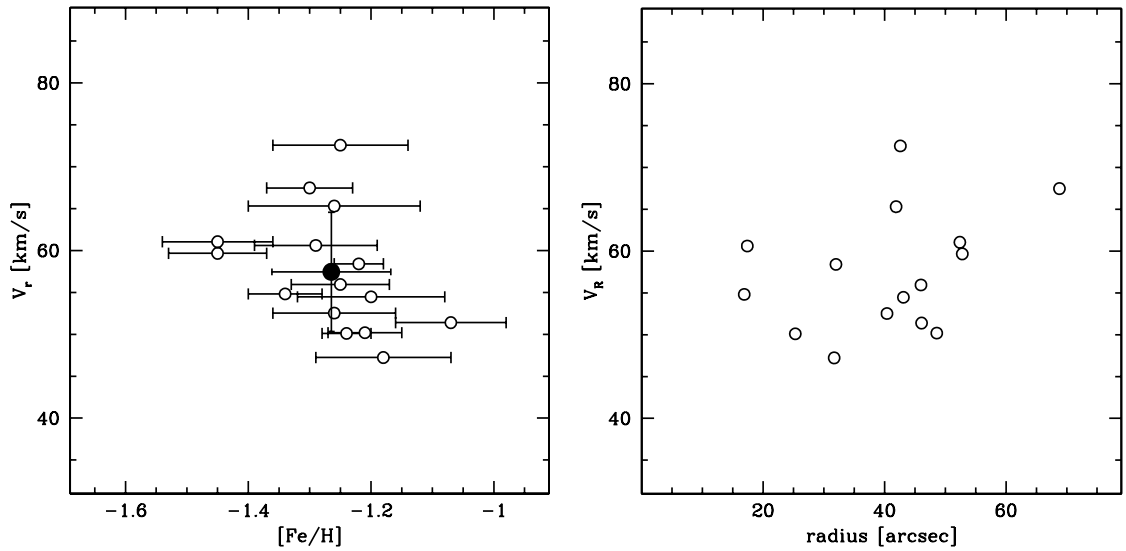

Fig. 4. Heliocentric radial velocities for the 15 stars likely cluster members as a function of metallicity (*left panel*) and distance form the cluster center (*right panel*). The big dot in the *left panel* indicates the average value and 1σ dispersion.

stars on a $2.5' \times 2'$ image taken with the LNA 1.6 m telescope. The membership of the eight stars in common based on derived radial velocities is consistent between the two studies with the only exception of star #14 (ID-I02:7), which according to I02 is a field star. However, in this case there might be a mismatch in the cross-identification of the observed star owing the presence of a nearby second source, which is clearly resolved in our SofI image (see Fig. 1), even better in the CRIRES acquisition camera, which has a resolution of 0.047″/pixel, but not as evident in the optical image shown in Fig. 1 of I02. Finally, because the position of star #14 in the optical CMD of I02 is not shown, we cannot rule out the hypothesis that we actually observed different stars. In contrast to what can be seen in our near-IR map, in the optical image of I02 star #14 and the nearby source appear to have comparable magnitude.

Nevertheless, what is most puzzling is the considerable disagreement on the derived radial velocities. Based on 11 probable cluster members out of a total of 17 observed stars, I02 found a mean radial velocity of $+114 \pm 14$ km s^{-1}, which is ∼60 km s^{-1} higher than our estimate based on a comparable sample. When we consider all the stars in common, but #14, there is an average difference of 69 km s^{-1} in the derived velocities and 1σ dispersion of 19 km s^{-1}. Our result is more consistent with a previous estimate based on integrated spectroscopy (Armandroff & Zinn 1988), which reported a mean velocity of +35 km s^{-1} although, admittedly, the integrated spectrum could have been heavily contaminated by the presence of bright field sources in the center.

After carefully checking the derived wavelength calibration of CRIRES spectra (see Sect. 2) we can rule out any systematic shift of ∼70 km s^{-1} in radial velocity. On the other hand, it could be that at much lower resolution, a possible mismatch of spectral features produces a substantial shift in the radial velocity measurements.

Our result is instead in good agreement with Vasquez et al. (in prep.), who derive a mean radial velocity of +65 km s^{-1} based on data obtained with FORS2 in multislit mode ($R \approx 2000$).

Despite the large difference in terms of spectral resolution between this work and I02, the metallicity estimates for the stars in common are reasonably consistent, within ∼0.3 dex, and ≤0.1 dex when stars #4 (ID-I02: 5) and #1 (ID-I02: 13) are excluded. However, despite being listed among the candidate cluster members, the metallicity tabulated by I02 for these two stars is 1 dex higher than the mean metallicity of Terzan 1 reported by the same authors. We found no obvious explaination for such a difference.

5. Conclusions

We have obtained high-resolution infrared spectroscopy of 16 giants in the heavily obscured Galactic GC Terzan 1. Based on the derived radial velocity estimates, 15 out of 16 observed giants turned out to be candidate cluster members. We measured a cluster mean heliocentric radial velocity of +57 km s^{-1} with 1σ dispersion of 7 km s^{-1}. This value is significantly less than what is reported in the Harris (1996) catalog based on the I02 study, but it is in good agreement with the most recent low-resolution optical estimate by Vasquez et al. (in prep.)

From our analysis of the candidate cluster members we find average [Fe/H] = -1.26 ± 0.03 dex, [O/Fe] = $+0.39 \pm 0.02$ dex, [Mg/Fe] = $+0.42 \pm 0.02$ dex, [Si/Fe] = $+0.31 \pm 0.05$ dex, and [Ti/Fe] = $+0.15 \pm 0.04$ dex. The derived metallicity estimates agree with the previous low-resolution optical spectroscopic study by I02, confirming that Terzan 1, the innermost cluster in the bulge direction, is metal-poor.

The [α/Fe] enhancement measured in Terzan 1 is fully consistent with those measured in other bulge clusters observed in near-IR by our group and in optical by other teams (see Valenti et al. 2011, and references therein), as well as with the estimate found in field giants located in the innermost bulge fields (Rich et al. 2012).

The derived iron content measured on Terzan 1 giants places this cluster on the metal-poor tail of the observed metallicity distribution function of the bulge field population (see Zoccali et al. 2008; Gonzalez et al. 2011; Johnson et al. 2011, 2013; Ness et al. 2013, and reference therein). Additionally, the observed α-enhancement makes Terzan 1 chemically similar to the cluster and field bulge metal-poor (i.e., [Fe/H] ∼ 1 dex) component.

Acknowledgements. E.V. warmly thanks the telescope operators and night astronomers of Paranal working on UT1, for their competence and dedication while doing observations for this program. R.M.R. acknowledges support from grants AST-1212095, AST-1413755 from the National Science Foundation.

The authors thank Ivo Saviane and Sergio Vasquez for sharing information on their results on Terzan 1 radial velocity measurements that will be presented in a forthcoming paper (Vasquez et al., in prep.). NSO/Kitt Peak FTS data used here were produced by NSF/NOAO.

References

Alves-Brito, A., Barbuy, B., Zoccali, M., et al. 2006, A&A, 460, 269
Armandrfoff, T. E., & Zinn, R. 1988, AJ, 96, 92
Barbuy, B., Renzini, A., Ortolani, S., et al. 1999, A&A, 341, 539
Barbuy, B., Zoccali, M., Ortolani, S., et al. 2006, A&A, 449, 349
Barbuy, B., Zoccali, M., Ortolani, S., et al. 2007, AJ, 134, 1613
Barbuy, B., Chiappini, C., Cantelli, E., et al. 2014, A&A, 570, A76
Biemont, E., & Grevesse, N. 1973, Atom. Data and Nucl. Data Tables, 12, 221
Carretta, E., Cohen, J. G., Gratton, R. G., Behr, B. 2001, AJ, 122, 1469
Carretta, E., Bragaglia, A., Gratton, R. G. et al., 2007, A&A, 464, 967
Cohen, J. G., Gratton, R. G., Behr, B., et al. 1999, ApJ, 523, 739
Gonzalez, O. A., Rejkuba, M., Zoccali, M., et al. 2011, A&A, 530, A54
Gratton, R. G., Sneden, C., & Carretta, E. 2004, ARA&A, 42, 385
Gratton, R. G., Lucatello, S., Bragaglia, A., et al. 2006, A&A, 455, 271
Grevesse, N., & Sauval, A. J. 1998, Space Sci. Rev., 85, 161
Idiart, T. P., Barbuy, B., Perrin, M. N., et al. 2002, A&A, 381, 472
Käufl, H. U., Ballester, P., Biereichel, P., et al. 2004, SPIE, 5492, 1218
Johnson, H. R., Bernat, A. P., & Krupp, B. M. 1980, ApJS, 42, 501
Johnson, C. I., Rich, R. M., Fullbright, J. P., et al. 2011, ApJ, 732, 108
Johnson, C. I., Rich, R. M., Kobayashi, C., et al. 2013, ApJ, 765, 157
Harris, W. E. 1996, AJ, 112, 1487
McLean, I., Becklin, E. E., Bendikoen, O., et al. 1998, SPIE, 3354, 566
McWilliam, A. 1997, ARA&A, 35, 503
Melendez, J., & Barbuy, B. 1999, ApJS, 124, 527
Montegriffo, P., Ferraro, F. R., Fusi Pecci, F., & Origlia, L. 1995, MNRAS, 276, 739
Ness, M., Freeman, K., Athanassoula, E., et al. 2013, MNRAS, 430, 836
Origlia, L., & Rich, R. M. 2004, AJ, 127, 3422
Origlia, L., Moorwood, A. F. M., & Oliva, E. 1993, A&A, 280, 536
Origlia, L., Ferraro, F. R., Fusi Pecci, F., & Oliva, E. 1997, A&A, 321, 859
Origlia, L., Rich, R. M., & Castro, S. 2002, AJ, 123, 1559
Origlia, L., Valenti, E., & Rich, R. M. 2005a, MNRAS, 356, 1276
Origlia, L., Valenti, E., Rich, R. M., & Ferraro, F. R. 2005b, MNRAS, 363, 897
Origlia, L., Valenti, E., & Rich, R. M. 2008, MNRAS, 388, 1419
Ortolani, S., Barbuy, B., Bica, E., et al. 1999, A&A, 350, 840
Rich, R. M., Origlia, L., & Valenti, E. 2012, ApJ, 746, 59
Valenti, E., Ferraro, F. R., & Origlia, L. 2010, MNRAS, 402, 1729
Valenti, E., Origlia, L., & Rich, R. M. 2011, MNRAS, 414, 2690
Zoccali, M., Barbuy, B., Hill, V., et al. 2004, A&A, 423, 507
Zoccali, M., Hill, V., Lecureur, A., et al. 2008, A&A, 486, 177